This article has been accepted for publication in a future issue of this journal, but has not been fully edited. Content may change prior to final publication. Citation information: DOI 10.1109/TSG.2017.2777738, IEEE Transactions on Smart Grid

Comprehensive Optimization Model for Sizing and Siting of DG Units, EV Charging Stations and Energy Storage Systems

Ozan Erdinç, *Senior Member, IEEE*, Akın Taşcıkaraoğlu, *Member, IEEE*, Nikolaos G. Paterakis, *Member, IEEE*, İlker Dursun, Murat Can Sinim, and João P. S. Catalão, *Senior Member, IEEE*

***Abstract*—The sizing and siting of renewable resources based distributed generation (DG) units has been a topic of growing interest, especially during the last decade due to the increasing interest in renewable energy systems and the possible impacts of their volatility on distribution system operation. This study goes beyond the existing literature by presenting a comprehensive optimization model for the sizing and siting of different renewable resources based DG units, electric vehicle (EV) charging stations and energy storage systems (ESSs) within the distribution system. The proposed optimization model is formulated as a second order conic programming problem, considering also the time-varying nature of DG generation and load consumption, in contrast with the majority of the relevant studies that have been based on static values.**

***Index Terms*—Distributed generation; distribution system; electric vehicle charging station; energy storage system; sizing and siting.**

NOMENCLATURE

The sets, parameters and decision variables that are used in this paper are alphabetically listed below in Tables I-III. Other symbols and abbreviations are defined where they first appear.

TABLE I. INDICES AND SETS

B^i	Set of MV buses.
B_l^{ij}	Set of lines where i is the sending and j is the receiving bus.
B_h^i	Set of LV buses and relevant MV/LV transformer units connected to MV bus i.
B_k^i	Set of sample load variations of EV charging stations.
h	Index of LV buses and relevant MV/LV transformer units.
i	Index of buses.
k	Index of sample load variations of EV charging stations.
t	Index of time periods.

TABLE II. PARAMETERS AND CONSTANTS

A, C	Binary numbers assigned for the structure of the objective function.
B_l	Susceptance of line l [pu].
CE^{ESS}	Charging efficiency of ESS.
DE^{ESS}	Discharging efficiency of ESS.
$M_{i,l}^F$	The coefficient that is 1 if bus i is the receiving end of line l, -1 if bus i is the sending end of line l, otherwise 0.
$M_{i,l}^L$	The coefficient that is 1 if bus i is the sending end of line l, otherwise 0.
$M_{l,i}^W$	The coefficient for bus i and line l obtained from the transpose of the matrix composed of $M_{i,l}^F$ values.
K	Allowance ratio of installed DG capacity within MV/LV transformer rated power.
k_1, k_2	Weighting coefficients.
$P_{EV\_CS,rated}$	EV charging station rated power [pu].
$P_{k,t}^{EV\_sample}$	Power demand in period t for sample load variation k of the EV charging station [pu].
$P_{h,i,t}^{L,LV\_other}$	Inelastic demand of LV bus h of MV bus i in period t [pu].
$P_{i,t}^{L,MV\_other}$	Inelastic demand of MV bus i connected directly from MV side in period t [pu].
$P_{\max @T_{ref}}$	Rated power of each reference PV panel at T_{ref} [pu].
$P_{PV\_ACT@T,h,i,t}$	Actual PV power production from each reference PV panel for LV bus h of MV bus i in period t [pu].
$P_{PV\_ACT@T,i,t}$	Actual PV power production from each reference PV panel for MV bus i in period t [pu].
$P_{wind,h,i,t}$	Actual wind power production from each reference wind turbine for LV bus h of MV bus i in period t [pu].
$P_{wind,i,t}$	Actual wind power production from each reference wind turbine for MV bus i in period t [pu].
$P_{wind,rated}$	Rated power of each reference wind turbine [pu].
$R^{ESS,ch}$	Charging rate of ESS [pu].
$R^{ESS,dis}$	Discharging rate of ESS [pu].
R_l	Resistance of line l [pu].
$Q_{i,t}^L$	Reactive power demand of MV bus i in period t [pu].
$SOE^{ESS,ini}$	Initial state-of-energy of ESS unit [pu].
$SOE^{ESS,max}$	Maximum state-of-energy of ESS unit [pu].
$SOE^{ESS,min}$	Minimum state-of-energy of ESS unit [pu].
$T_{i,t}$	Temperature variation within the region of MV bus i in period t [^{0}C].
T_{ref}	Reference temperature for PV panel (usually considered as 25^{0}C) [^{0}C].
$Temp\_coeff_{P_{max}}$	Temperature coefficient defined by manufacturer for modeling the impact of temperature change on PV power production [%/^{0}C].
$TR_{h,i}^{lim}$	Rated power of MV/LV transformer between MV bus i and LV bus h [pu].
$v_{i,t}$	Wind speed variation within the region of MV bus i in period t [m/s].
V_{max}	Maximum allowed voltage level for MV buses [pu].
V_{min}	Minimum allowed voltage level for MV buses [pu].
$ł_{ACT,i,t}$	Solar radiation variation within the region of MV bus i in period t [W/m^2].
$ł_{REF}$	Reference solar radiation for PV panel (usually considered as 1000 W/m^2) [W/m^2].
ΔT	Time granularity [h].

This work was supported by Energy Market Regulatory Authority of Turkey (EPDK) R&D Funds (project "Impact Analysis and Optimization Project of Systems Embedded to Distribution System-DAGSIS"), by FEDER funds through COMPETE 2020 and by Portuguese funds through FCT, under Projects SAICT-PAC/0004/2015 - POCI-01-0145-FEDER-016434, POCI-01-0145-FEDER-006961, UID/EEA/50014/2013, UID/CEC/50021/2013, UID/EMS/00151/2013 and SFRH/BPD/103744/2014. Also, the research leading to these results has received funding from the EU Seventh Framework Programme FP7/2007-2013 under grant agreement no. 309048 (project SiNGULAR).

O. Erdinç is with the Department of Electrical Engineering, Yildiz Technical University, Istanbul, Turkey (e-mail: oerdinc@yildiz.edu.tr). O. Erdinç is also with INESC-ID, Instituto Superior Técnico, University of Lisbon, Lisbon 1049-001, Portugal.

A. Tascikaraoglu is with the Department of Electrical and Electronics Engineering, Mugla Sitki Kocman University, Mugla, Turkey (e-mail: akintascikaraoglu@mu.edu.tr).

N. G. Paterakis is with the Department of Electrical Engineering, Eindhoven University of Technology (TU/e), PO Box 513, 5600 MB Eindhoven, The Netherlands (e-mail: n.paterakis@tue.nl).

İ. Dursun and M. C. Sinim are with the R&D department of Bogazici Electric Distribution Company (BEDAS), Istanbul, Turkey (e-mails: ilker.dursun@bedas.com.tr; murat.sinim@bedas.com.tr).

J.P.S. Catalão is with INESC TEC and the Faculty of Engineering of the University of Porto, Porto 4200-465, Portugal, also with C-MAST, University of Beira Interior, Covilhã 6201-001, Portugal, and also with INESC-ID, Instituto Superior Técnico, University of Lisbon, Lisbon 1049-001, Portugal (e-mail: catalao@ubi.pt).

This article has been accepted for publication in a future issue of this journal, but has not been fully edited. Content may change prior to final publication. Citation information: DOI 10.1109/TSG.2017.2777738, IEEE Transactions on Smart Grid

TABLE III. DECISION VARIABLES

$E_i^{ESS\_cap}$	Total capacity of ESS unit of MV bus i.
$n_{EV\_CS,k,h,i}$	Number of EV charging stations installed within LV bus h of MV bus i for sample EV load k.
$n_{LV\_ESS,h,i}$	Number of reference ESS units installed within LV bus h of MV bus i.
$n_{LV\_PV,h,i}$	Number of reference PV panels installed within LV bus h of MV bus i.
$n_{LV\_wind,h,i}$	Number of reference wind turbines installed within LV bus h of MV bus i.
$n_{MV\_PV,i}$	Number of reference PV panels installed directly connected to MV bus i.
$n_{MV\_wind,i}$	Number of reference wind turbines installed directly connected to MV bus i.
$P_i^{DG\_cap}$	Total DG capacity for MV bus i.
$P_{h,i}^{DG\_cap\_LV}$	DG capacity for LV bus h of MV bus i.
$P_i^{DG\_cap\_MV}$	DG capacity directly connected to MV bus i.
$P_{h,i,t}^{ESS,ch}$	Charging power of ESS unit connected to LV bus h of MV bus i in period t [pu].
$P_{h,i,t}^{ESS,dis}$	Discharging power of ESS unit connected to LV bus h of MV bus i in period t [pu].
$P_i^{EV\_CS\_cap}$	Total EV charging station capacity for MV bus i.
$P_{i,t}^{G}$	Power available at MV bus i in period t [pu].
$P_{i,t}^{L}$	Total load of MV bus i in period t [pu].
$P_{h,i,t}^{L,EV}$	Total EV charging based power consumption for LV bus h of MV bus i in period t [pu].
$P_{l,t}^{loss}$	Active power loss of line l in period t [pu].
$\hat{P}_{l,t}^{loss}$	Model variable to represent the active power loss of line l in period t [pu].
$P_{h,i,t}^{LV-}$	Total power drawn by LV bus h from MV bus i in period t [pu].
$P_{h,i,t}^{LV+}$	Total power injected by LV bus h to MV bus i in period t [pu].
$P_{h,i,t}^{LV\_DG}$	Total DG power production for LV bus h of MV bus i in period t [pu].
$P_{h,i,t}^{LV\_PV}$	Total PV power production for LV bus h of MV bus i in period t [pu].
$P_{h,i,t}^{LV\_wind}$	Total wind power production for LV bus h of MV bus i in period t [pu].
$P_{i,t}^{MV\_DG}$	Total DG power production directly injected to MV bus i in period t [pu].
$P_{i,t}^{MV\_PV}$	Total PV power production directly injected to MV bus i in period t [pu].
$P_{i,t}^{MV\_wind}$	Total wind power production directly injected to MV bus i in period t [pu].
$P_{l,t}^{r}$	Active power flow at receiving end of line l in period t [pu].
$P_{i,t}^{S}$	Substation supply at bus i in period t [pu].
$Q_{l,t}^{loss}$	Reactive power loss of line l in period t [pu].
$Q_{i,t}^{G}$	Reactive power generated/consumed at bus i in period t[pu].
$Q_{l,t}^{r}$	Reactive power flow at receiving end of line l in period t [pu].
$SOE_{h,i,t}^{ESS}$	State-of-energy of ESS unit connected to LV bus h of MV bus i in period t [pu].
$V_{i,t}$	Voltage magnitude at bus i in period t [pu].
$W_{i,t}$	Square of the voltage magnitude at bus i in period t [pu].
$W_{r,t}$	Square of the voltage magnitude at receiving bus r ($r \in i$) in period t [pu].
$u_{h,i,t}^{1}$	Binary variable of logical constraints for the power decomposition of LV bus h.
$u_{h,i,t}^{2}$	Binary variable for ESS model. 1 if ESS unit connected to LV bus h of MV bus i is charging in period t, otherwise 0.

I. INTRODUCTION

A. Motivation and Background

IN alignment with the raising environmental concerns, the economic and political risks posed by the scarcity of fossil fuels and the technological advances during the last decades, the investments on renewable energy resources have significantly increased, promoted by the incentives offered by the governments of both developed and developing countries. Although relying on such resources presents environmental advantages and increases self-sufficiency, there are also severe drawbacks that can challenge the traditional operational and planning procedures of electric power systems. The most significant disadvantage is that the majority of renewable energy resources, including wind and solar power production, are highly volatile and non-dispatchable because of their dependence on meteorological conditions [1], [2]. Thus, the system operators (SOs) should carefully take into account this high variability especially in the case of power systems with significant penetration of renewable energy systems [3].

In particular, the distribution system has a more vulnerable structure compared to transmission system, and the increase in the integration of renewable energy sources in the form of distributed generation (DG) units needs proper planning actions from the SO side. In the same time, the demand side has recently shown a considerable change due to the uptake of a new generation of electric loads. For instance, electric vehicles (EVs) have significant levels of power requirements as a load (e.g. 7.4 kW for BMW i3 regular charger [4], 19.2 kW for Tesla Home Charging Station [5], 22 kW for Renault ZOE Medium Charger [6], 43 kW for Renault ZOE Fast Charger [6], 120 kW for Tesla SuperCharger [7], etc.) and a vital potential as a mobile storage unit via the Vehicle-to-Grid (V2G) operation mode with considerable battery capacities (e.g. 33 kWh for BMW i3 [4], 100 kWh for Tesla Model X [8], etc.). Moreover, the introduction of distributed energy storage systems (ESSs) within the distribution system has been also recognized by SOs as a means of enhancing the operational flexibility [9], [10].

Considering all the aforementioned elements the planning of investments in renewable based DG units and the integration of new technologies, such as EVs and ESSs, at the demand side is a prevalent issue and the need for distribution SO to rely on comprehensive sizing and siting methodologies is rendered evident.

B. Literature Overview

There are several studies that deal with the sizing and siting of DG units. Among them, Moradi and Abedini [11] solved the power loss minimization and voltage stability maximization oriented multi-objective DG sizing-siting problem in distribution system using a combined genetic algorithm and particle swarm optimization based approach. Kefayat et al. [12] proposed a multi-objective DG sizing-siting problem simultaneously considering the minimization of losses, cost and emissions, as well as the maximization of the voltage stability index. The contribution of [12] was the consideration of the uncertainty pertaining wind production and load consumption. Kaur et al. [13], proposed a sequential siting and capacity planning model using a Mixed Integer Nonlinear Programming (MINLP) context aiming to minimize distribution system losses. Medina et al. [14] developed an investment and operational cost minimization oriented Mixed Integer Linear Programming (MILP) model for the DG sizing and siting problem in radial distribution systems. Foster et al. [15] compared MILP and genetic algorithm (GA) methods for the DG sizing and siting problem in terms of computational performance. Sheng et al. [16] proposed an improved solution technique for multi-objective DG sizing and siting, targeting at minimum line losses and voltage deviation, as well as maximum stability. Pereira et al. [17] considered the sizing and siting of both DG units and capacitor banks within a distribution system and adopted a Tabu search and GA based hybrid solution technique, considering also the stochasticity in

This article has been accepted for publication in a future issue of this journal, but has not been fully edited. Content may change prior to final publication. Citation information: DOI 10.1109/TSG.2017.2777738, IEEE Transactions on Smart Grid

power production of DG units. Ameli et al. [18] combined the DG owner and distribution company point of view in a multi-objective optimization context solved by particle swarm optimization (PSO). Kroposki et al. [19] proposed a feeder ranking based approach for renewable DG sizing and siting in distribution systems.

Two different studies considering the sizing and siting of EV charging stations and ESS units within the distribution system without taking DG units into account can be found in [20] and [21]. Lastly, a comprehensive literature study considering the sizing and siting of both DG units and EV charging stations was provided in [22]. More detailed reviews dedicated to this topic can be found in [23]-[26].

It should be noted that, in general, distribution system planning problems consider investment, replacement, maintenance and other operational costs. However, sizing and siting oriented distribution system problems are generally different than the regular distribution system planning problems. The main idea behind sizing and siting approaches is to determine the optimal capacity of DG and other technologies that can be installed in the distribution system without hampering its tight operational limits. Thus, in such studies the perspective of the SO is adopted in order to determine limits to a possible additional production/consumption units based private investment in terms of DG units, EV charging stations, etc. at a particular connection point within the distribution system, such that operational limits are not violated. Besides, SO based investments such as common ESS units to increase the operational flexibility from SO point of view can also be analyzed combined with the impacts of aforementioned possible private investments within such conceptual analyses.

C. Content and Contributions

In this study, an optimal sizing and siting approach formulated as a second order conic programming problem, simultaneously considering wind and solar energy based DG units, EV charging stations and ESS units is proposed.

The novel points of the proposed study compared to the existing literature can be listed as follows:

- To the best knowledge of the authors, this is the first literature study that co-optimizes the size and location of different renewable-based DG units, EV charging stations and ESS units.
- Unlike several studies that consider only static values for generation and consumption, this study simultaneously considers time-varying profiles of load demand, DG production and EV based charging demand in order to address temporal mismatches between the production of DG units and load consumption.

D. Organization of the paper

The remainder of the paper is organized as follows: in Section II the proposed methodology is described in detail. Results are presented and discussed in Section III. Finally, conclusions are drawn and directions for future studies are provided in Section IV.

II. METHODOLOGY

The proposed methodology aims to determine the optimum size of DG (photovoltaics - PV, wind), EV charging station and ESS penetration within the distribution system. Figure 1 presents a MV bus that connects directly DG units and loads, as well as LV buses where relatively smaller loads, DG and ESS units are connected.

The objective function of the optimization problem is represented by (1). As described by (1), the objective can either be minimizing the total losses ($A = 1, C = 0$), maximizing the total DG, EV charging station and ESS penetration within the distribution system ($A = 0, C = 0$) or a multi-objective combination of both ($A = 0, C = 1$).

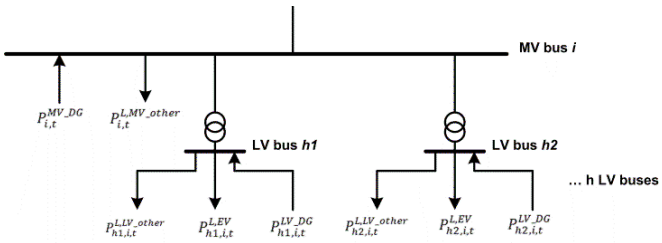

Figure 1. Schematic of a MV bus considered in this study.

$$\begin{aligned} Minimize\ L = {} & A \cdot \left(\sum_t \sum_l \hat{P}_{l,t}^{loss} \right) \\ & - (1 - A) \cdot \sum_i \left(P_i^{DG_{cap}} + P_i^{EV_{CS_{cap}}} + E_i^{ESS_{cap}} \right) \\ & + C \cdot \left(\sum_t \sum_l k_1 \cdot \hat{P}_{l,t}^{loss} - k_2 \right. \\ & \left. \cdot \left[P_i^{DG_{cap}} + P_i^{EV_{CS_{cap}}} + E_i^{ESS_{cap}} \right] \right) \end{aligned} \quad (1)$$

The constraints of the problem are expressed by (2)-(34).

$$P_{i,t}^G - P_{i,t}^L = \sum_{l \in B_l^{ij}} \left(M_{i,l}^F \cdot P_{l,t}^r + M_{i,l}^L \cdot P_{l,t}^{loss} \right) \ \forall i, t \quad (2)$$

$$\begin{aligned} Q_{i,t}^G - Q_{i,t}^L = {} & \sum_{l \in B_l^{ij}} \left(M_{i,l}^F \cdot Q_{l,t}^r + M_{i,l}^L \cdot Q_{l,t}^{loss} - B_l \cdot M_{l,i}^W \right. \\ & \left. \cdot W_{i,t} \right) \ \forall i, t \end{aligned} \quad (3)$$

$$P_{i,t}^G = P_{i,t}^S + P_{i,t}^{MV\_DG} + \sum_{h \in B_h^i} P_{h,i,t}^{LV+} \ \forall i, t \quad (4)$$

$$P_{i,t}^L = P_{i,t}^{L,MV\_other} + \sum_{h \in B_h^i} P_{h,i,t}^{LV-} \ \forall i, t \quad (5)$$

$$W_{i,t} = V_{i,t}^2 \ \forall i, t \quad (6)$$

$$P_{l,t}^{loss} = 2 \cdot R_l \cdot \hat{P}_{l,t}^{loss} \forall l, t \quad (7)$$

$$X_l \cdot P_{l,t}^{loss} - R_l \cdot Q_{l,t}^{loss} = 0 \ \forall l, t \quad (8)$$

$$\begin{aligned} \sum_i \left(M_{l,i}^W \cdot W_{i,t} \right) = {} & 2 \cdot R_l \cdot P_{l,t}^r + 2 \cdot X_l \cdot Q_{l,t}^r + R_l \cdot P_{l,t}^{loss} \\ & + X_l \cdot Q_{l,t}^{loss} \forall l, t \end{aligned} \quad (9)$$

$$2 \cdot \hat{P}_{l,t}^{loss} \cdot W_{r,t} \geq {P_{l,t}^r}^2 + {Q_{l,t}^r}^2 \forall l, t \quad (10)$$

$$V_{min}^2 \leq W_{i,t} \leq V_{max}^2 \ \forall i, t \quad (11)$$

Constraints (2) and (3) stand for the active and reactive power balance at each MV bus. Equation (4) decomposes the power that is available at each MV bus to the contribution of the DG units directly connected to MV bus, the injection at substation buses, and the power injected by the excess power of LV buses. Similarly, (5) enforces the fact that the system load comprises inelastic demand, and the power deficit of LV

This article has been accepted for publication in a future issue of this journal, but has not been fully edited. Content may change prior to final publication. Citation information: DOI 10.1109/TSG.2017.2777738, IEEE Transactions on Smart Grid

buses. The equality constraints (6)-(10) enforce relationships between substitute variables in order to obtain a simpler AC power flow representation as derived directly from [27] with relevant adjustments. It should be noted that a power flow representation in conic format is adopted in this study due to its capabilities of achieving high-accuracy modeling compared to DC power flow model, and of obtaining a relatively simpler power flow representation compared to full AC power flow model. Furthermore, the iteration numbers in these models are generally very low and do not change considerably with the increasing size of the network, which enables these models to be used effectively for practical implementations. The relevant representation for the power flow concept can also be followed from Fig. 2. Besides, (11) constrains the voltage at each bus to be between allowable lower and upper limits.

The power decomposition and the logical constraints regarding the power balance at each LV bus are represented by (12)-(14).

$$P_{h,i,t}^{LV\_DG} + P_{h,i,t}^{ESS,dis} - P_{h,i,t}^{L,LV_{other}} - P_{h,i,t}^{L,EV} - P_{h,i,t}^{ESS,ch} = P_{h,i,t}^{LV+} - P_{h,i,t}^{LV-} \quad (12)$$

$$P_{h,i,t}^{LV+} \le TR_{h,i}^{lim} \cdot u_{h,i,t}^{1} \quad (13)$$

$$P_{h,i,t}^{LV-} \le TR_{h,i}^{lim} \cdot \left(1 - u_{h,i,t}^{1}\right) \quad (14)$$

The decomposition of total DG power injected directly to MV bus consists of possible PV and wind turbine (WT) installations as in (15).

$$P_{i,t}^{MV\_DG} = P_{i,t}^{MV\_PV} + P_{i,t}^{MV\_wind} \quad (15)$$

The PV power for each reference PV panel is calculated regarding the temperature variation and solar irradiation as in (16).

$$P_{PV\_ACT@T,i,t} = \frac{Ɨ_{ACT,i,t}}{Ɨ_{REF}} = \frac{\left(T_{i,t} - T_{ref}\right) \cdot Temp\_coeff_{P_{max}} + 100}{100} \cdot P_{\max @T_{ref}} \quad (16)$$

where the reference solar irradiation and temperature values are 1000 $\mathrm{W/m^2}$ and 25^0C, respectively. Thus, the PV power injected directly to each MV bus is calculated by (17).

$$P_{i,t}^{MV\_PV} = n_{MV\_PV,i} \cdot P_{PV\_ACT@T,i,t} \quad (17)$$

The wind power each WT with rated power of $P_{wind,rated}$ is obtained as a function of the wind speed as in (18), where the power curves of specific WT types can be employed in this regard.

$$P_{wind,i,t} = f\left(v_{i,t}\right) \quad (18)$$

Thus, the wind power injected directly to each MV bus is calculated by (19).

$$P_{i,t}^{MV\_wind} = n_{MV\_wind,i} \cdot P_{wind,i,t} \quad (19)$$

Similar expressions can be derived for LV bus DG installations as in (20)-(22), assuming that the same PV panel and WT is used in the installation and the meteorological conditions — and as a result the power variations of reference PV panels and WTs — in different regions of the same bus are identical, i.e., $P_{PV\_ACT@T,i,t} = P_{PV\_ACT@T,h,i,t}$, $P_{wind,i,t} = P_{wind,h,i,t}$.

$$P_{h,i,t}^{LV\_DG} = P_{h,i,t}^{LV\_PV} + P_{h,i,t}^{LV\_wind} \quad (20)$$

$$P_{h,i,t}^{LV\_PV} = n_{LV\_PV,h,i} \cdot P_{PV\_ACT@T,h,i,t} \quad (21)$$

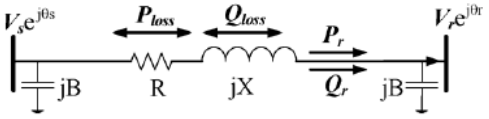

Figure 2. Line model [27].

$$P_{h,i,t}^{LV\_wind} = n_{LV\_wind,h,i} \cdot P_{wind,i,t} \quad (22)$$

The total installed DG capacity connected at each LV bus h is calculated by (23).

$$P_{h,i}^{DG\_cap\_LV} = n_{LV\_PV,h,i} \cdot P_{\max @T_{ref}} + n_{LV\_wind,h,i} \cdot P_{wind,rated} \quad (23)$$

In some countries, regulations limit the total installed DG capacity at LV side to be below a ratio of the rated MV/LV transformer capacity (e.g. in Turkey, the relevant regulation states that the total installed DG capacity should not exceed 30% of the relevant MV/LV transformer's rated power). This is enforced by (24).

$$P_{h,i}^{DG\_cap\_LV} \le K \cdot TR_{h,i}^{lim} \quad (24)$$

Similar to (23), the total installed DG capacity directly connected at each MV bus i is calculated by (25).

$$P_{i}^{DG\_cap\_MV} = n_{MV\_PV,i} \cdot P_{\max @T_{ref}} + n_{MV\_wind,i} \cdot P_{wind,rated} \quad (25)$$

Thus, the total DG capacity from both the MV and LV side for each MV bus i can be obtained by (26).

$$P_{i}^{DG\_cap} = P_{i}^{DG\_cap\_MV} + \sum_{h \in B_h^i} P_{h,i}^{DG\_cap\_LV} \quad (26)$$

The EV charging load at each LV bus h should be also derived. Considering only a single type of charging station type for the sake of simplicity, k types of sample load variations can be defined considering the physical usage of the EV charging station which can differ regarding the actual area the charging station is placed (in a household, in a working place, etc.) and the charging habits of the EV owners. Thus, the EV charging load at each LV bus h is obtained by defining the number of identical charging stations of sample load variation k can be placed at each LV bus h in (27).

$$P_{h,i,t}^{L,EV} = \sum_{k \in B_k^i} n_{EV\_CS,k,h,i} \cdot P_{k,t}^{EV\_sample} \quad (27)$$

Thus, the total EV charging station capacity for each MV bus i is calculated by (28).

$$P_{i}^{EV\_CS\_cap} = P_{EV\_CS,rated} \cdot \sum_{h \in B_h^i} \sum_{k \in B_k^i} n_{EV\_CS,k,h,i} \quad (28)$$

Finally, the ESS model considered in this study is represented by (29)-(33) [28]. Eqs. (29) and (30) limit the ESS charging and discharging rate together with logical constraints on charging and discharging power. State-of-energy (SOE) of ESS is considered by (31) and (32) while it is bounded by lower and upper limits using (33). Finally, the total capacity of ESS unit of MV bus i is calculated by (34).

$$0 \le P_{h,i,t}^{ESS,ch} \le R^{ESS,ch} \cdot u_{h,i,t}^{2}, \forall t \quad (29)$$

$$0 \le P_{h,i,t}^{ESS,dis} \le R^{ESS,dis} \cdot (1 - u_{h,i,t}^{2}), \forall t \quad (30)$$

This article has been accepted for publication in a future issue of this journal, but has not been fully edited. Content may change prior to final publication. Citation information: DOI 10.1109/TSG.2017.2777738, IEEE Transactions on Smart Grid

$$SOE_{h,i,t}^{ESS} = SOE_{h,i,t-1}^{ESS} + CE^{ESS} \cdot P_{h,i,t}^{ESS,ch} \cdot \Delta T - \frac{P_{h,i,t}^{ESS,dis}}{DE^{ESS}} \cdot \Delta T, \forall t \geq 1 \quad (31)$$

$$SOE_{h,i,t}^{ESS} = n_{LV\_ESS,h,i} \cdot SOE^{ESS,ini}, if\ t = 1 \quad (32)$$

$$n_{LV\_ESS,h,i} \cdot SOE^{ESS,min} \leq SOE_{h,i,t}^{ESS} \leq n_{LV\_ESS,h,i} \cdot SOE^{ESS,max}, \forall t \quad (33)$$

$$E_i^{ESS\_cap} = \sum_{h \in B_h^i} n_{LV\_ESS,h,i} \cdot SOE^{ESS,max} \quad (34)$$

It should be also noted that this problem can be discretized into sub-problems of either sizing or siting respectively considering the sites or sizes for implementation as known parameters. The proposed formulation can therefore be manipulated in this manner either considering the size or site information as an input data instead of a decision variable.

III. Tests And Results

A. Input Data

The proposed approach is tested on two real distribution system feeders in Istanbul, namely the Alibeykoy and Hadimkoy feeders. The line parameters and transformer data of the Alibeykoy feeder are presented in Tables IV and V, while the relevant data for the Hadimkoy feeder are given in Tables VI and VII.

For the mentioned feeders, the yearly inflexible consumption data of the buses with the lowest and highest peak power demand are given in Figs. 3-6 due to space limitations. It should be noted that the time granularity of the available data and also the simulation studies is 0.5h (30mins). Besides, the relevant meteorological data including temperature, solar radiation and wind speed variations are presented in Figs. 7-9 respectively. Here it should be also stated that for the relevant parameters of PV panel, the specifications of the 250 W industrial PV panel that were given in [29] are utilized.

The EV consumption profiles are obtained experimentally using charging data of a BMW i3 as shown in Fig. 10 for a normal charging station.

Three different profiles are provided for normal and fast charging stations as follows: 1) Type-1/K1, normal charging station – workplace load, 2) Type-1/K2, normal charging station – residential neighborhood load, 3) Type-2/K1, fast charging station (obtained via normalization of time and power values for normal charging station data) – a common place (such as a gas station) load profile. The relevant profiles are presented in Figs. 11-13.

B. Simulation and Results

The model was coded in GAMS 24.0.2 and has been solved by the commercial solver MOSEK. Six different cases are evaluated for both Alibeykoy and Hadimkoy feeders:

- *Case-1:* ESS available, objective function is to minimize losses;
- *Case-2:* ESS available, objective function is to maximize DG, EV charging station and ESS capacity;
- *Case-3:* ESS available, objective function is both to minimize losses and maximize DG, EV charging station and ESS capacity;
- *Case-4:* ESS unavailable, objective function is to minimize losses;
- *Case-5:* ESS unavailable, objective function is to maximize DG and EV charging station capacity;
- *Case-6:* ESS unavailable, objective function is both to minimize losses and maximize DG and EV charging station capacity.

TABLE IV. ALIBEYKOY FEEDER LINE PARAMETERS

	From	To	R [pu]	X [pu]	B [pu]
L1	n1	n0	0.00015	0.000244	0.080639
L2	n2	n1	6.47E-05	0.000106	0.034815
L3	n3	n2	6.47E-05	0.000106	0.034937
L4	n3	n4	5.71E-05	9.33E-05	0.030783
L5	n4	n5	2.86E-05	5.46E-05	0.017975
L6	n5	n6	2.44E-05	4.7E-05	0.01542
L7	n7	n6	2.44E-05	4.62E-05	0.015374
L8	n7	n8	3.28E-05	5.38E-05	0.017657
L9	n9	n8	2.52E-05	4.03E-05	0.013406
L10	n9	n10	4.79E-05	7.81E-05	0.025921
L11	n11	n10	4.2E-05	6.89E-05	0.022762

TABLE V. MV/LV TRANSFORMER CAPACITIES OF ALIBEYKOY FEEDER

	Transformer Power [kVA]		Transformer Power [kVA]
n11	630	**n5**	1250x2 (2 LV buses exist)
n10	1600	**n4**	1000
n9	1000	**n3**	1000
n8	1000	**n2**	1250
n7	1600	**n1**	630
n6	630		

TABLE VI. HADIMKOY FEEDER LINE PARAMETERS

	From	To	R [pu]	X [pu]	B [pu]
L1	100	0	5.88E-05	0.00015	0.061173
L2	100	103	0.000121	0.000294	0.03076
L3	100	132	0.000477	0.001111	0.034754
L4	100	144	0.00048	0.001152	0.461362
L5	143	144	3.53E-05	3.78E-05	0.009826
L6	142	143	6.3E-05	6.89E-05	0.017663
L7	141	142	4.7E-05	5.12E-05	0.013294
L8	140	141	0.000133	0.000145	0.037351
L9	100	147	0.000501	0.001214	0.485938
L10	137	138	8.65E-05	9.41E-05	0.024293
L11	138	139	3.11E-05	3.36E-05	0.008657
L12	139	140	7.23E-05	7.81E-05	0.020214
L13	147	149	4.2E-06	4.2E-06	0.001102
L14	147	148	6.72E-06	7.56E-06	0.001857

TABLE VII. MV/LV TRANSFORMER CAPACITIES OF HADIMKOY FEEDER

	Transformer Power [kVA]		Transformer Power [kVA]
n140	1250	**n137**	1250
n141	1000	**n149**	1600
n142	1250	**n148**	1600
n143	1250	**n147**	1600
n144	630	**n103**	400
n139	1600	**n132**	1000
n138	1600	**n100**	1000

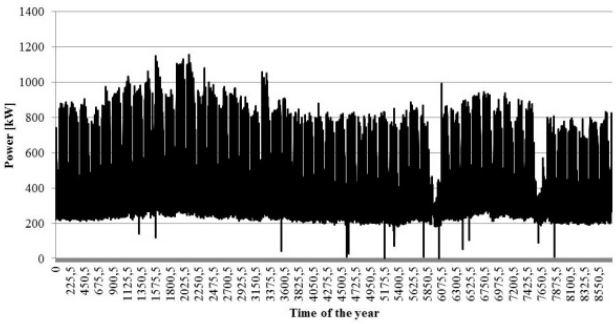

Figure 3. The yearly power consumption profile of the bus with the highest peak demand (n2) for Alibeykoy feeder.

This article has been accepted for publication in a future issue of this journal, but has not been fully edited. Content may change prior to final publication. Citation information: DOI 10.1109/TSG.2017.2777738, IEEE Transactions on Smart Grid

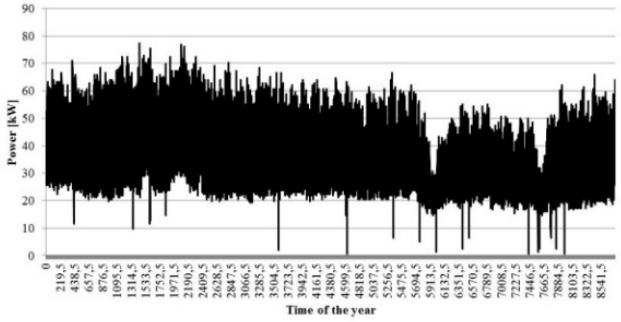

Figure 4. The yearly power consumption profile of the bus with the lowest peak demand (n4) – Alibeykoy feeder.

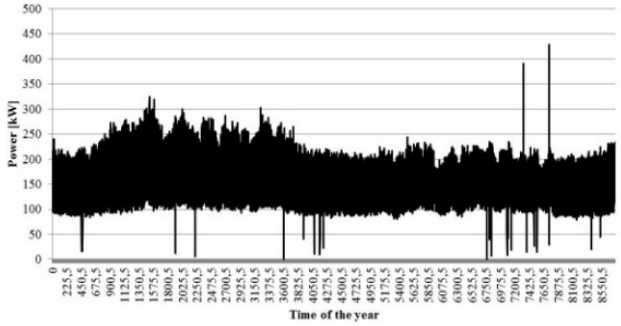

Figure 5. The yearly power consumption profile of the bus with the highest peak demand (n140) – Hadimkoy feeder.

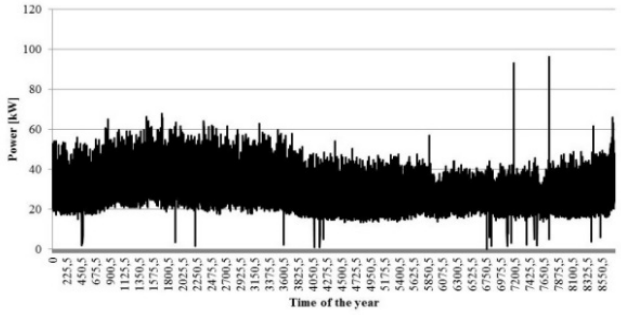

Figure 6. The yearly power consumption profile of the bus with the lowest peak demand (n144) – Hadimkoy feeder.

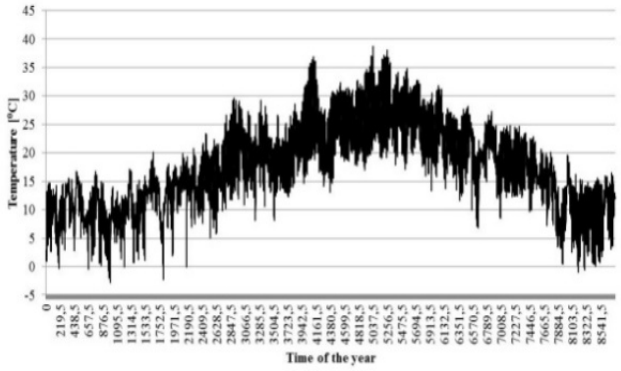

Figure 7. Yearly temperature variation.

It should be noted that for Cases 3 and 6, the weighting coefficients in Eq. (1) are both considered equal to one. The obtained sizing and siting results are given in detail in Tables VIII and IX respectively for Alibeykoy and Hadimkoy feeders. It should be noted that Type-1 for the considered WT corresponds to 200 kW rated power, while Type-2 corresponds to 50 kW. The minimum voltage among all buses and total active power losses for both feeders are also summarized in Table X. Note that the minimum voltage value of each bus at each time step does not decrease below the predefined minimum voltage, which is 0.9 pu, for all the cases considered. In Table X, the percentage of active power losses is calculated by the division of total load energy consumption via EV charging, inflexible loads and ESS charging by the total energy drawn through the distribution lines from the connection point of the relevant feeder to the main distribution system.

As seen from the obtained results, the approach maximizes the ESS capacity during the availability of ESS as the capital cost required for ESS investment, etc. is not considered. The availability of ESS generally results in lower active power losses and increased DG and EV charging station capacities. Here, the change of the objective function especially affects the obtained results during the ESS unavailability conditions. The choice of a multi-objective concept instead of solely considering loss minimization results in a slightly increase in total losses in turn of increasing DG and EV charging station capacities. It should be stated here that the mentioned percentage of losses does not consider many other factors and therefore presented just for comparison purposes. In reality, the transformer losses, the LV line losses, etc. factors are non-negligible and the percentage of losses therefore will be greater together with these impacts.

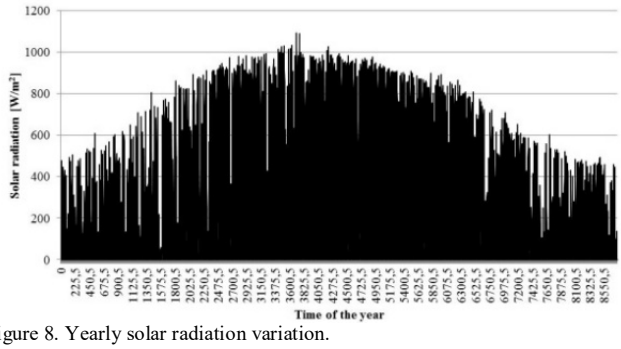

Figure 8. Yearly solar radiation variation.

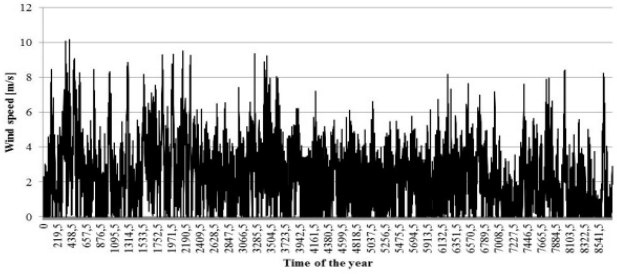

Figure 9. Yearly wind speed variation.

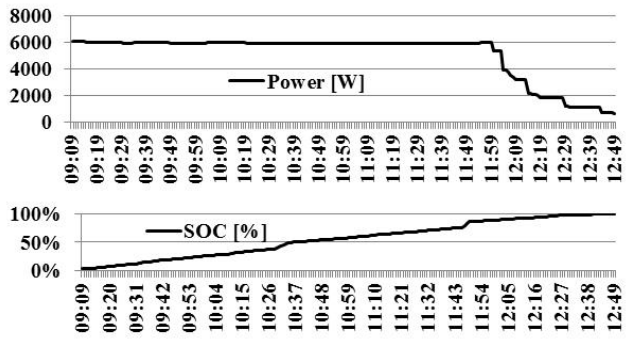

Figure 10. The experimental charging data for BMW i3.

This article has been accepted for publication in a future issue of this journal, but has not been fully edited. Content may change prior to final publication. Citation information: DOI 10.1109/TSG.2017.2777738, IEEE Transactions on Smart Grid

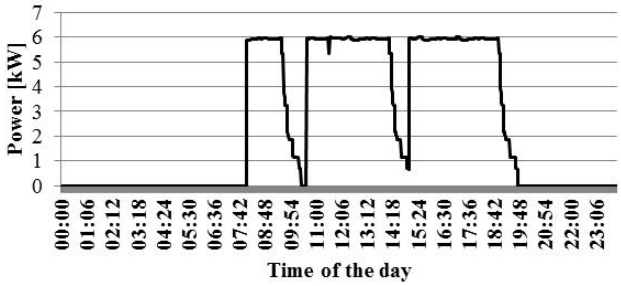

Figure 11. The power demand curve of EV charging for Type-1/K1.

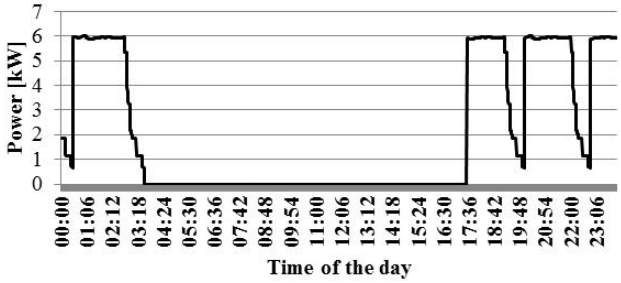

Figure 12. The power demand curve of EV charging for Type-1/K2.

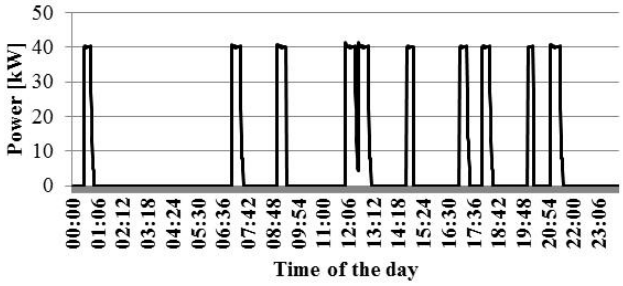

Figure 13. The power demand curve of EV charging for Type-2/K1.

In order to clearly observe the benefits of the ESS and DG units to the operation of the distribution system, various analyses are also presented on a higher-resolution scale for Alibeykoy feeder. With this objective, two different typical days that reflect the frequently encountered generation and consumption profiles in the considered area are chosen. It should be noted that only the buses with the highest renewable generation and power consumption are considered first and among them the ones having the data with the maximum standard deviation, namely buses n10, n5, n3 and n2, are shown in the related figures in order to avoid data redundancy.

TABLE VIII. THE RESULTS OF DIFFERENT CASES FOR ALIBEYKOY FEEDER

Bus	PV power [kW]	WT power [kW]	N. of WT		N. of EV charging stat.			ESS cap. [kWh]	PV power [kW]	WT power [kW]	N. of WT		N. of EV charging stat.			ESS cap. [kWh]
					Type-1		Type-2						Type-1		Type-2	
			Type-1 [50 kW]	Type-2 [200 kW]	K1 [7.4 kW]	K2 [7.4 kW]	K1 [50 kW]				Type-1 [50 kW]	Type-2 [200 kW]	K1 [7.4 kW]	K2 [7.4 kW]	K1 [50 kW]	
	Case-1								Case-2							
n11	25	150	0	3	0	0	0	100	0	0	0	0	39	25	1	100
n10	25	450	2	1	0	0	0	100	50	400	2	0	78	48	6	100
n9	0	100	0	2	0	0	0	100	125	0	0	0	58	64	5	100
n8	0	250	0	5	0	0	0	100	25	0	0	0	40	55	2	100
n7	25	450	0	9	0	0	0	100	25	400	2	0	77	95	2	100
n6	125	0	0	0	1	0	0	100	0	0	0	0	40	41	1	100
n5	100	1350	5	7	87	0	0	200	575	800	4	0	119	130	41	200
n4	0	50	0	1	0	0	0	100	25	0	0	0	21	93	1	100
n3	50	300	0	6	0	0	0	100	25	200	0	4	86	0	0	100
n2	25	350	1	3	0	0	0	100	100	50	0	1	49	38	0	100
n1	25	150	0	3	0	0	0	100	0	100	0	2	31	34	2	100
	Case-3								Case-4							
n11	25	150	0	3	0	0	0	100	0	150	0	3	0	0	0	-
n10	25	450	2	1	0	0	0	100	0	250	1	1	0	0	0	-
n9	0	100	0	2	0	0	0	100	0	100	0	2	0	4	0	-
n8	0	250	0	5	0	0	0	100	0	300	1	2	0	2	0	-
n7	25	450	2	1	0	0	0	100	25	450	2	1	0	0	0	-
n6	0	50	0	1	0	0	0	100	50	50	0	1	0	0	0	-
n5	0	1400	5	8	87	0	0	200	0	1300	6	2	25	0	0	-
n4	0	50	0	1	0	0	0	100	0	50	0	1	0	0	0	-
n3	0	300	0	6	0	0	0	100	0	300	0	6	0	0	0	-
n2	25	350	1	3	0	0	0	100	0	350	1	3	1	0	0	-
n1	25	150	0	3	0	0	0	100	25	150	0	3	0	0	0	-
	Case-5								Case-6							
n11	25	50	0	1	18	32	2	-	0	150	0	3	0	0	0	-
n10	200	250	0	5	59	69	0	-	0	250	1	1	0	0	0	-
n9	50	50	0	1	68	28	4	-	0	100	0	2	4	4	0	-
n8	0	0	0	0	46	44	5	-	0	300	1	2	0	2	0	-
n7	150	200	1	0	95	16	0	-	25	450	2	1	0	0	0	-
n6	25	0	0	0	26	16	1	-	50	50	0	1	0	0	0	-
n5	25	1300	4	10	134	50	71	-	0	1300	6	2	25	0	0	-
n4	0	100	0	2	93	66	2	-	0	50	0	1	0	0	0	-
n3	150	50	0	1	53	32	3	-	0	300	0	6	0	0	0	-
n2	75	250	0	5	32	25	5	-	0	350	1	3	1	0	0	-
n1	25	50	0	1	27	6	6	-	25	150	0	3	0	0	0	-

TABLE IX. THE RESULTS OF DIFFERENT CASES FOR HADIMKOY FEEDER

Bus	PV power [kW]	WT power [kW]	N. of WT		N. of EV charging stat.			ESS cap. [kWh]	PV power [kW]	WT power [kW]	N. of WT		N. of EV charging stat.			ESS cap. [kWh]
			Type-1 [50 kW]	Type-2 [200 kW]	Type-1 K1 [7.4 kW]	Type-1 K2 [7.4 kW]	Type-2 K1 [50 kW]				Type-1 [50 kW]	Type-2 [200 kW]	Type-1 K1 [7.4 kW]	Type-1 K2 [7.4 kW]	Type-2 K1 [50 kW]	
	Case-1								Case-2							
n140	0	100	0	2	0	0	0	100	250	100	0	2	76	33	6	92
n141	0	200	1	0	8	0	0	100	100	200	1	0	69	63	2	92
n142	0	100	0	2	0	0	0	100	25	100	0	2	13	79	3	91
n143	0	200	1	0	6	0	0	93	25	0	0	0	71	69	6	92
n144	0	50	0	1	3	0	0	91	0	50	0	1	44	28	4	91
n139	0	200	1	0	35	0	0	95	175	0	0	0	50	30	1	93
n138	0	150	0	3	1	0	0	100	25	0	0	0	24	28	0	93
n137	0	200	1	0	17	0	0	100	25	50	0	1	94	13	0	93
n149	0	200	1	0	40	0	0	94	100	0	0	0	13	57	0	93
n148	25	200	1	0	5	4	0	97	250	100	0	2	68	22	15	100
n147	0	200	1	0	43	0	0	100	50	0	0	0	51	17	16	91
n103	0	100	0	2	0	0	0	94	100	0	0	0	0	12	1	100
n132	0	300	1	2	0	0	0	92	0	300	0	6	1	43	0	100
n100	0	200	1	0	1	0	0	90	25	150	0	3	1	6	15	100
	Case-3								Case-4							
n140	0	300	1	2	1	0	0	100	0	250	1	1	0	0	0	-
n141	0	200	1	0	7	0	0	100	0	100	0	2	0	0	0	-
n142	0	100	0	2	0	0	0	99	25	100	0	2	1	0	0	-
n143	0	200	1	0	5	0	0	100	0	200	1	0	21	0	0	-
n144	0	50	0	1	5	0	0	99	75	0	0	0	8	2	0	-
n139	0	200	1	0	35	0	0	100	0	100	0	2	3	0	0	-
n138	0	150	0	3	1	0	0	100	0	150	0	3	1	3	1	-
n137	0	200	1	0	17	0	0	100	125	0	0	0	8	1	0	-
n149	0	200	1	0	44	0	0	100	0	100	0	2	0	0	0	-
n148	25	200	1	0	5	4	0	100	25	200	1	0	23	7	0	-
n147	0	200	1	0	38	0	0	100	0	100	0	2	8	0	0	-
n103	0	100	0	2	0	0	0	100	0	0	0	0	2	1	0	-
n132	0	300	1	2	0	0	0	100	0	300	1	2	3	0	0	-
n100	0	200	1	0	1	0	0	100	0	200	1	0	2	0	1	-
	Case-5								Case-6							
n140	25	0	0	0	53	37	1	-	0	250	1	1	0	0	0	-
n141	0	250	0	5	78	29	1	-	0	100	0	2	0	0	0	-
n142	200	100	0	2	89	36	7	-	25	100	0	2	1	0	0	-
n143	100	150	0	3	85	31	8	-	0	200	1	0	21	0	0	-
n144	25	0	0	0	53	0	1	-	75	0	0	0	8	2	0	-
n139	0	50	0	1	16	63	0	-	0	100	0	2	3	0	0	-
n138	0	100	0	2	97	38	9	-	0	150	0	3	1	3	1	-
n137	75	150	0	3	84	29	3	-	125	0	0	0	8	1	0	-
n149	25	150	0	3	55	72	12	-	0	100	0	2	0	0	0	-
n148	0	250	1	1	44	99	14	-	25	200	1	0	23	7	0	-
n147	50	50	0	1	23	41	28	-	0	100	0	2	8	0	0	-
n103	0	0	0	0	24	15	1	-	0	0	0	0	2	1	0	-
n132	0	100	0	2	100	13	1	-	0	300	1	2	3	0	0	-
n100	275	0	0	0	60	26	7	-	0	200	1	0	2	0	1	-

The power generation values of PV panels and wind turbines that have the maximum capacities for the predetermined buses given in Table VIII for case 1 are shown in Figs. 15 and 16 for the first day considered. It should be noted that the same characteristics with different power levels are obtained for different buses as the same types of PV panel and wind turbine are considered in the test cases. As seen from Figs. 1 and 2, a considerable amount of renewable energy, which is 801.3 kWh and 18332.1 kWh for solar power and wind power from all the buses respectively, is supplied to the distribution system, which prevents the active power losses that are likely to be faced on both transmission and distribution lines. More importantly, these DG units connected to the optimum buses with the appropriate power rating values enable power-intensity loads such as EVs to be connected to the distribution systems with the minimum power losses and without being affected by the LV transformer power capacity limits. A high number of EVs can thus be connected to the distribution system and even charged at the same time, as seen from Fig. 17 that shows the load demand of LV buses including the EV charging loads.

During various time periods, the renewable power generation can be low when the total load demand is very high. For such cases, the ESS units have the capability of providing a portion of these demands, which both decreases the resulting power losses caused by the transmission of the required energy from grid to the loads and helps the voltage level remain in the allowable limits. As seen from Figs. 15, 16 and 17, such a case is encountered between 18:00 and 19:00 and during this peak demand period, the ESS units connected to different buses support the distribution system as much as possible as shown in Fig. 18 while limiting the power drawn from the grid through the LV transformer. The buses to which the power from the available ESS units will be injected are determined based on the load demand of the buses, voltage levels of the buses and also the factors influencing the total power losses such as the impedance between the buses.

Regarding the latter representative day, similar generation and consumption profiles can be observed from Figs. 19-22. As a difference from the first day, the generation from the DG units is much higher in this case for almost the same

This article has been accepted for publication in a future issue of this journal, but has not been fully edited. Content may change prior to final publication. Citation information: DOI 10.1109/TSG.2017.2777738, IEEE Transactions on Smart Grid

consumption values. Therefore, the ESS units are charged with the excess power frequently compared to the case for the first day. The lower initial capacities of these units are also the other reason for these more frequent charge-discharge interactions.

TABLE X. MINIMUM VOLTAGE AND ACTIVE POWER LOSSES VALUES OBTAINED FOR BOTH FEEDERS

Case	Alibeykoy		Hadimkoy	
	Min. voltage [pu]	Percentage of power losses [%]	Min. voltage [pu]	Percentage of power losses [%]
Case-1	0.998	0.086	0.999	0.054
Case-2	0.936	6.278	0.925	3.404
Case-3	0.998	0.085	0.999	0.054
Case-4	0.998	0.085	0.999	0.059
Case-5	0.930	6.524	0.921	3.482
Case-6	0.998	0.085	0.999	0.059

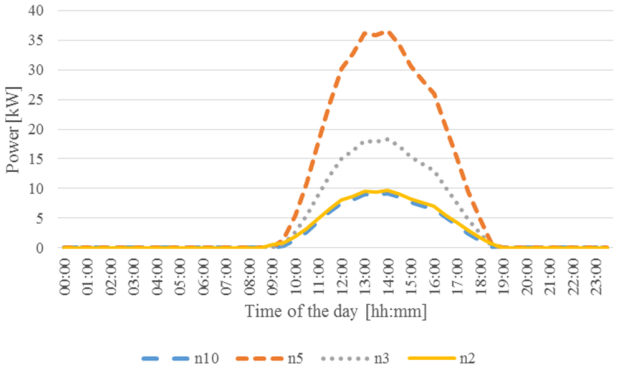

Figure 15. Daily power curve of PV panels connected to different buses for the first day considered.

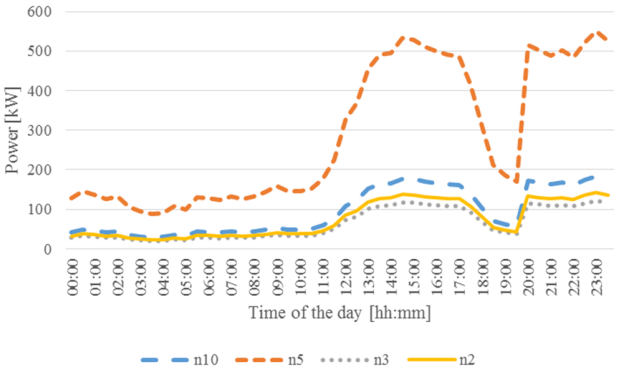

Figure 16. Daily power curve of wind turbines connected to different buses for the first day considered.

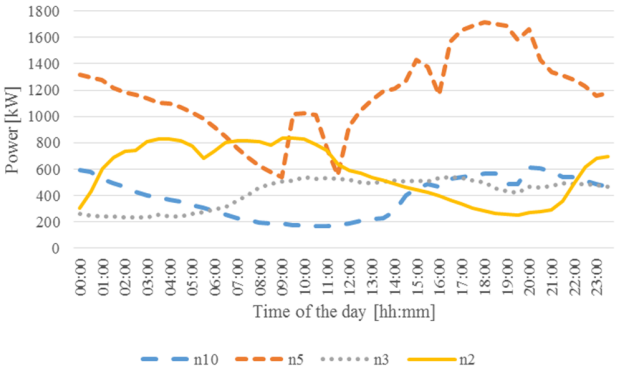

Figure 17. Daily LV load demand curve connected to different buses for the first day considered.

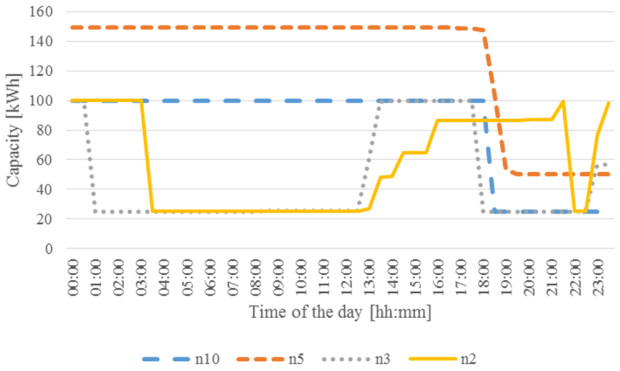

Figure 18. Daily capacity curve of storage systems connected to different buses for the first day considered.

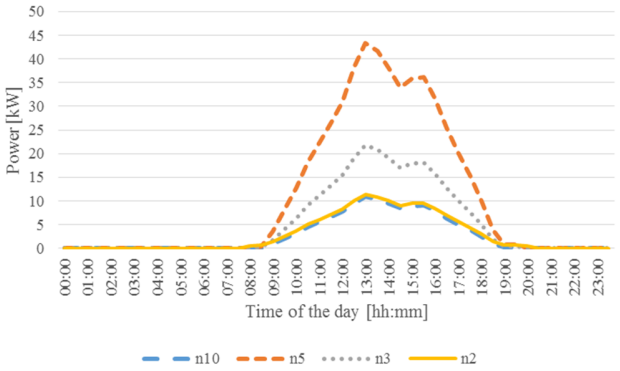

Figure 19. Daily power curve of PV panels connected to different buses for the second day considered.

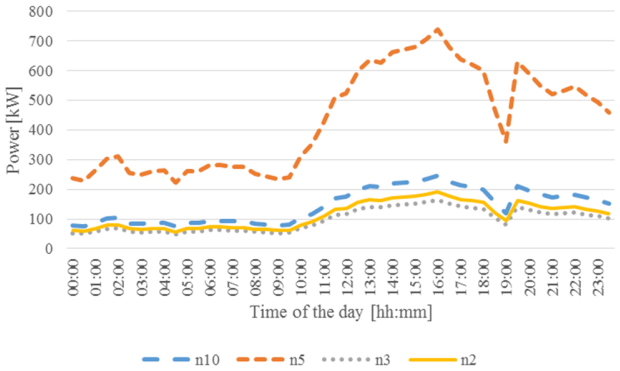

Figure 20. Daily power curve of wind turbines connected to different buses for the second day considered.

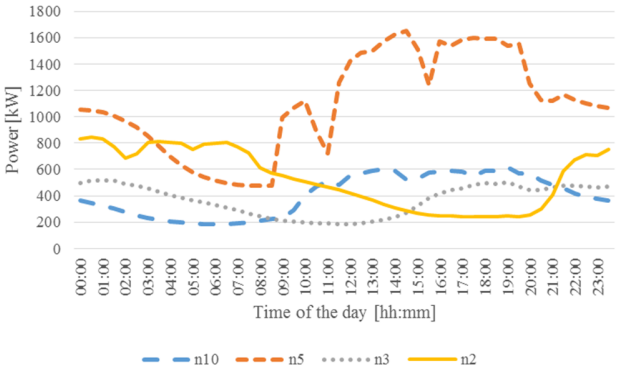

Figure 21. Daily LV load demand curve connected to different buses for the second day considered.

This article has been accepted for publication in a future issue of this journal, but has not been fully edited. Content may change prior to final publication. Citation information: DOI 10.1109/TSG.2017.2777738, IEEE Transactions on Smart Grid

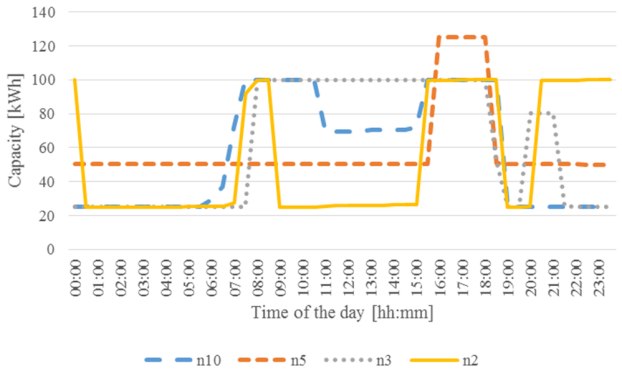

Figure 22. Daily capacity curve of storage systems connected to different buses for the second day considered.

C. The User Interface

The aforementioned concept normally needs deep understanding of the given formulation in Section II and the understanding of the code written in GAMS. However, in normal conditions, the technical staff of a SO company can be non-expert in these issues, although the technical requirements and the results can be well-analyzed on the basis of their technical knowledge. Therefore, an easy-to-use user interface for SO is also developed in using Java. Following the installation of the program, the user selects the Excel file that includes the input parameters to the program in a relevant and explained format by a prepared User's Guide as seen in Fig. 14. Then, the user simply needs to click the Run button and the GAMS code in the back-end is executed, while the solution progress and finally the output of the simulation results can be followed by the pop-up screens as shown in Fig. 15. The main screen also shows a brief and useful summary of the obtained results where the pop-up Excel folder shows further results in a more detailed version. The graphical user interface has a modular structure where the written GAMS code and all other details can be changed, revised and upgraded easily by following the available User's Guide.

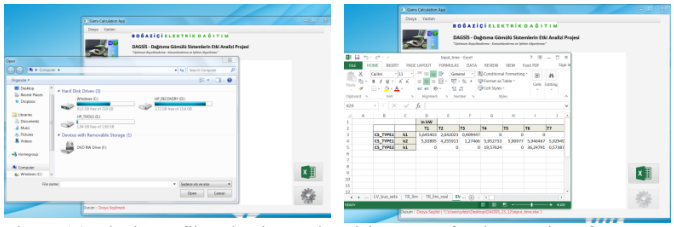

Figure 14. The input file selection and revision stage for the user interface.

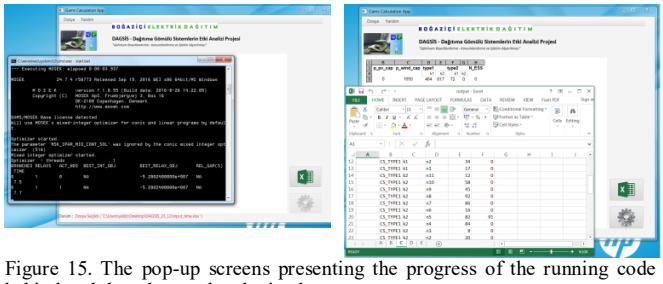

Figure 15. The pop-up screens presenting the progress of the running code behind and then the results obtained.

IV. Conclusions

In this study, a new concept simultaneously considering the sizing and siting of wind and solar based renewable DG units, EV charging stations of different types serving multiple types of end-users and ESS units for distribution systems was proposed. The proposed approach considered the time dependency of DG based power production and EV and other loads based consumption, on the contrary to the majority of the literature that neglected the time-varying nature of the mentioned factors. Comprehensive simulations were conducted with the real distribution system and load data of BEDAS for two different real distribution system parts of Istanbul, Turkey. Besides, an SO interface for non-expert users of the proposed algorithmic structure was developed.

The future studies on this topic can consider the possible flexibility of loads with demand response strategies. Besides, the stochasticity regarding several parameters such as DG based production, EV (regarding plug-in times, arrival SoE values and desired departure SoE values) and other loads based consumption can also be taken into account by transforming the proposed formulation into a stochastic programming concept. Moreover, the investment, replacement and maintenance costs of SO owned assets such as ESS units rather than private investment related costs can also be considered in the planning problem in upcoming studies.

V. References

[1] N. Li, C. Uckun, E. M. Constantinescu, J. R. Birge, K. W. Hedman, and A. Botterud, "Flexible operation of batteries in power system scheduling with renewable energy," *IEEE Trans. Sustainable Energy*, vol. 7, pp. 685-696, Apr. 2016.

[2] A. Tascikaraoglu, B. M. Sanandaji, G. Chicco, V. Cocina, F. Spertino, O. Erdinc, N. G. Paterakis, and J. P. S. Catalão, "Compressive Spatio-Temporal Forecasting of Meteorological Quantities and Photovoltaic Power," *IEEE Trans. Sust. Energy*, vol. 7, pp. 1295-1305, July 2016.

[3] N. G. Paterakis, O. Erdinc, A. G. Bakirtzis, and J.P.S. Catalao, "Qualification and quantification of reserves in power systems under high wind generation penetration considering demand response," *IEEE Trans. Sustainable Energy*, vol. 6, pp. 88-103, Jan. 2015.

[4] *BMW i3 Specifications*[Online]. Available: http://www.plugincars.com/bmw-i3.html

[5] *Tesla Home Charging Station Specifications*[Online]. Available: https://www.tesla.com/support/home-charging-installation#technical-specs

[6] *Renault ZOE Specifications*[Online]. Available: https://www.renault.ie/vehicles/new-vehicles/zoe/battery-and-charging.html

[7] *TeslaSuperChargerSpecifications*[Online]. Available: https://www.tesla.com/supercharger

[8] *Tesla Model X Specifications*[Online]. Available: https://www.tesla.com/modelx

[9] X. Shen, M. Shahidehpour, Y. Han, S. Zhu, and J. Zheng, "Expansion planning of active distribution networks with centralized and distributed energy storage systems,"*IEEE Trans. Sustainable Energy*, vol. 8, pp. 126-134, Jan. 2017.

[10] N. Jayasekara, M. A. S. Masoum, and P. J. Wolfs, "Optimal operation of distributed energy storage systems to improve distribution network load and generation hosting capability," *IEEE Trans. Sustainable Energy*, vol. 7, pp. 250-261, Jan. 2016.

[11] M. H. Moradi, and M. Abedini, "A combination of genetic algorithm and particle swarm optimization for optimal DG location and sizing in distribution systems," *Electrical Power and Energy Systems*, vol. 34, pp. 66-74, Jan. 2012.

[12] M. Kefayat, A. L. Ara, and S. A. N. Niaki, "A hybrid of ant colony optimization and artificial bee colony algorithm for probabilistic optimal placement and sizing of distributed energy resources," *Energy Conversion and Management*, vol. 92,pp. 149-161, Mar. 2015.

[13] S. Kaur, G. Kumbhar, and J. Sharma, "A MINLP technique for optimal placement of multiple DG units in distribution systems," *Int. J. Electr. Power and Energy Syst.*, vol. 63 pp. 609-617, Dec. 2014.

[14] A. C. R. Medina, J. F. Franco, M. J. Rider, A. P. Feltrin, and R. Romero, "A mixed-integer linear programming approach for optimal type, size and allocation of distributed generation in radial distribution systems," *Electric Power Systems Research*, vol. 97, pp.133-143, Apr. 2013.

[15] J. D. Foster, A. M. Berry, N. Boland, and H. Waterer, "Comparison of mixed-integer programming and genetic algorithm methods for distributed generation planning," *IEEE Trans. Power Systems*, vol. 29, pp. 833-843, Mar. 2014.

[16] W. Sheng, K. Y. Liu, Y. Liu, X. Meng, and Y. Li, "Optimal placement and sizing of distributed generation via an improved nondominated sorting genetic algorithm II," *IEEE Trans. Power Delivery*, vol. 30, pp. 569-, Apr. 2015.

[17] B. R. Pereira Jr., G. R. M. da Costa, J. Contreras, and J. R. S. Mantovani, "Optimal distributed generation and reactive power allocation in electrical distribution systems," *IEEE Trans. Sustainable Energy*, vol. 7, pp. 975-984, July 2016.

[18] A. Ameli, S. Bahrami, F. Khazeli, and M. R. Haghifam, "A multiobjective particle swarm optimization for sizing and placement of DGs from DG owner's and distribution company's viewpoints," *IEEE Trans. Power Delivery*, vol. 29, pp. 1831-1840, Aug. 2014.

[19] B. Kroposki, P. K. Sen, and K. Malmedal, "Optimum sizing and placement of distributed and renewable energy sources in electric power distribution systems," *IEEE Trans. Industry Applications*, vol. 49, pp. 2741-2752, Nov./Dec. 2013.

[20] A. El-Zonkoly, and L. D. S. Coelho, "Optimal allocation, sizing of PHEV parking lots in distribution system," *Int. J. Electr. Power and Energy Syst.*, vol. 67 pp. 472-477, May 2015.

[21] M. Nick, R. Cherkaoui, and M. Paolone, "Optimal siting and sizing of distributed energy storage via alternating direction method of multipliers," *Int. J. Electr. Power and Energy Syst.*, vol. 78, pp. 33-39, Nov. 2015.

[22] Z. Liu, F. Wen, and G. Ledwich, "Optimal siting and sizing of distributed generators in distribution systems considering uncertainties," *IEEE Trans. Power Delivery*, vol. 26, pp.2541-2551, Oct. 2011.

[23] P. Prakash, and D. K. Khatod, "Optimal sizing and siting techniques for distributed generation in distribution systems: A review," *Renewable and Sustainable Energy Reviews*, vol. 57, pp. 111-130, May 2016.

[24] M. Pesaran, P. D. Huy, V. K. Ramachandaramurthy, "A review of the optimal allocation of distributed generation: Objectives, constraints, methods, and algorithms," *Renew. Sust. Energy Reviews*, 2017, in press.

[25] W. L. Theo, J. S. Lim, W. S. Ho, H. Hashim, C. T. Lee, "Review of distributed generation (DG) system planning and optimization techniques: Comparison of numerical and mathematical modelling methods," *Renew. Sust. Energy Reviews*, vol. 67, pp. 531-573, Jan. 2017.

[26] P. S. Georgilakis, and N. Hatziargyriou, "Optimal distributed generation placement in power distribution networks: Models, methods, and future research," *IEEE Trans. Power Systems*, vol. 28, pp. 3420-3428, Aug. 2013.

[27] M. Baradar, and M. R. Hesamzadeh, "AC power flow representation in conic format," *IEEE Trans. Power Systems*, vol. 30, pp. 546-547, Jan. 2015.

[28] O. Erdinc, N.G. Paterakis, T.D.P. Mendes, A.G. Bakirtzis, and J.P.S. Catalao, "Smart household operation considering bi-directional EV and ESS utilization by real-time pricing-based DR," *IEEE Trans. Smart Grid*, vol. 6, pp. 1281-1291, May 2015.

[29] *Mitsubishi 250 W Monocrystalline PV PanelSpecifications*[Online]. Available:https://www.mitsubishi-electric.co.nz/materials/solar/brochures/PV-MLT_series_monocrystalline.pdf

BIOGRAPHIES

Ozan Erdinç (M'14-SM'16) received the B.Sc., M.Sc., and Ph.D. degrees from Yildiz Technical University (YTU), Istanbul, Turkey, in 2007, 2009, and 2012, respectively. Until May 2013, he worked in the private sector in different positions including electrical installations, renewable energy investments and as procurement expert. In June 2013, he became a Postdoctoral Fellow with the University of Beira Interior, Covilhã, Portugal, under the EU-FP7 funded Project "Smart and Sustainable Insular Electricity Grids Under Large-Scale Renewable Integration". Later, he joined the Department of Electrical Engineering, YTU, Istanbul, where in April 2016 he obtained the title of *Doçent Dr.* (Associate Prof. Dr.). He is currently also a Researcher with the INESC-ID, Lisbon, Portugal. His research interests are hybrid renewable energy systems, electric vehicles, power system operation, and smart grid technologies.

Akın Taşcıkaraoğlu (S'12-M'14) received the B.Sc., M.Sc., and Ph.D. degrees from Yildiz Technical University, Istanbul, Turkey, in 2006, 2008, and 2013, respectively. From February 2012 to October 2017 he was a researcher in the Department of Electrical Engineering, Yildiz Technical University, Istanbul. Also, he was a Postdoctoral Scholar at the University of California, Berkeley from April 2013 to April 2014. He is currently an Assistant Professor with the Department of Electrical and Electronics Engineering, Mugla Sitki Kocman University, Mugla. His research interests include among others forecasting, renewable energy, power system operation, smart grid, and demand response.

Nikolaos G. Paterakis (S'14-M'15) received the Dipl. Eng. degree from the Department of Electrical and Computer Engineering, Aristotle University of Thessaloniki, Thessaloniki, Greece in 2013 and the Ph.D. degree from the University of Beira Interior, Covilhã, Portugal in 2015. From October 2015 to March 2017 he was a Post-Doctoral Fellow with the Department of Electrical Engineering, Eindhoven University of Technology, Eindhoven, The Netherlands, where he is currently an Assistant Professor. His research interests include power systems operation and planning, renewable energy integration, ancillary services, demand response and smart grid applications.

İlker Dursun received his B.Sc. degree in 2003, M.Sc. degree in 2006 from Sakarya University, TURKEY and his PhD degree at Yildiz Technical University in 2016. He has been working at Bogazici Electricity Distribution Company for more than 11 years at different departments and duties. Now he is working as Investment and R&D Director. His main interests are power systems, smart grid applications, distributed generation, switching optimization, balanced-unbalanced load flow analysis, technical/non-technical loss analysis.

Murat Can Sinim received the B.Sc. degree from Istanbul University, in 2013 and he is currently studying MBA at Bahcesehir University, Turkey. He has been working at Bogazici Electricity Company for more than 2 years at R&D department as a R&D Engineer, and now he is working as R&D Manager. His main interests are, load flow analysis, technical/non-technical loss analysis, data mining, power system analysis.

João P. S. Catalão (M'04-SM'12) received the M.Sc. degree from the Instituto Superior Técnico (IST), Lisbon, Portugal, in 2003, and the Ph.D. degree and Habilitation for Full Professor ("Agregação") from the University of Beira Interior (UBI), Covilha, Portugal, in 2007 and 2013, respectively.

Currently, he is a Professor at the Faculty of Engineering of the University of Porto (FEUP), Porto, Portugal, and Researcher at INESC TEC, INESC-ID/IST-UL, and C-MAST/UBI. He was the Primary Coordinator of the EU-funded FP7 project SiNGULAR ("Smart and Sustainable Insular Electricity Grids Under Large-Scale Renewable Integration"), a 5.2-million-euro project involving 11 industry partners. He has authored or coauthored more than 575 publications, including 200 journal papers (more than 50 IEEE Transactions/Journal papers), 330 conference proceedings papers, 31 book chapters, and 14 technical reports, with an *h*-index of 34, an *i10*-index of 123, and over 5100 citations (according to Google Scholar), having supervised more than 50 post-docs, Ph.D. and M.Sc. students. He is the Editor of the books entitled *Electric Power Systems: Advanced Forecasting Techniques and Optimal Generation Scheduling* and *Smart and Sustainable Power Systems: Operations, Planning and Economics of Insular Electricity Grids* (Boca Raton, FL, USA: CRC Press, 2012 and 2015, respectively). His research interests include power system operations and planning, hydro and thermal scheduling, wind and price forecasting, distributed renewable generation, demand response and smart grids.

Prof. Catalão is an Editor of the IEEE TRANSACTIONS ON SMART GRID, an Editor of the IEEE TRANSACTIONS ON SUSTAINABLE ENERGY, an Editor of the IEEE TRANSACTIONS ON POWER SYSTEMS, and an Associate Editor of the *IET Renewable Power Generation*. He was the Guest Editor-in-Chief for the Special Section on "Real-Time Demand Response" of the IEEE TRANSACTIONS ON SMART GRID, published in December 2012, and the Guest Editor-in-Chief for the Special Section on "Reserve and Flexibility for Handling Variability and Uncertainty of Renewable Generation" of the IEEE TRANSACTIONS ON SUSTAINABLE ENERGY, published in April 2016. Since May 2017, he is the Corresponding Guest Editor for the Special Section on "Industrial and Commercial Demand Response" of the IEEE TRANSACTIONS ON INDUSTRIAL INFORMATICS. He was the recipient of the 2011 Scientific Merit Award UBI-FE/Santander Universities and the 2012 Scientific Award UTL/Santander Totta, in addition to an Honorable Mention in the 2017 Scientific Awards ULisboa/Santander Universities. Moreover, he has won 4 Best Paper Awards at IEEE Conferences.